Published in IET Communications
Received on 2nd October 2012
Revised on 9th February 2013
Accepted on 15th March 2013
doi: 10.1049/iet-com.2012.0600

ISSN 1751-8628

Effect of avalanche photodiode and thermal noises on the performance of binary phase-shift keying-subcarrier-intensity modulation/free-space optical systems over turbulence channels

Duy A. Luong, Truong C. Thang, Anh T. Pham

Computer Communications Laboratory, University of Aizu, Fukushima, Japan
E-mail: pham@u-aizu.ac.jp

Abstract: In this study, the authors theoretically study the performance of direct-detection free-space optical communication systems using binary phase-shift keying subcarrier-intensity modulation and avalanche photodiode (APD). The system bit-error rate and channel capacity are theoretically derived in cases of log-normal and gamma-gamma channel models for weak-to-moderate and moderate-to-strong atmospheric turbulence conditions, respectively. The authors quantitatively discuss the optimal values of the APD average gain, required transmitted optical power, and operating bit-rate considering various turbulence conditions, APD shot noise and thermal noise. It is seen that, although the impact of turbulence is severe, a proper selection of APD average gain could significantly improve the system performance in both cases of turbulence channels. The optimal value of APD average gain remains almost the same for different levels of turbulence; nevertheless it varies significantly in accordance to the change of receiver noise temperature.

1 Introduction

Free-space optical (FSO) communications, also known as wireless optical communications, has recently received a noticeable attention as an alternative to broadband wireless communications [1–3]. Besides its significant advantages of cost-effectiveness, quick and easy deployment and high-speed connections, the FSO communications also offers a solution to the problem of spectrum scarcity, especially in the wireless-access environment.

One of the major challenges in FSO systems under clear air conditions is the atmospheric turbulence, which is caused by refractive-index variations of the air along the transmission path. The atmospheric turbulence causes the random intensity fluctuation of the received optical signal, also known as scintillation effect, which severely degrades the system performance. So far, several atmospheric turbulence channel models have been proposed, of which log-normal and gamma–gamma models are the most commonly used for the cases of weak-to-moderate and moderate-to-strong turbulences, respectively. Previous works showed that they provided a good agreement between theoretical and experimental data [2, 4–7].

Conventionally, on–off keying (OOK) intensity modulation scheme is preferred thanks to its simplicity and low cost [1]. OOK systems however require an adaptive threshold to optimally operate in atmospheric turbulence conditions [8]. This brings more challenge to the system design as the OOK receiver will need knowledge of both noise level and turbulence state. As an alternative to the OOK, binary phase-shift keying subcarrier-intensity modulation (BPSK-SIM) scheme was first proposed in [9] and its performance over log-normal turbulence channel was comprehensively analysed [7, 10]. It is seen that, compared to OOK, BPSK-SIM is more suitable for FSO systems thanks to the use of 'zero' threshold level. In [11], the performance of BPSK-SIM/FSO systems using an array of n-PIN photodetectors has been reported. Compared to the single-photodetector systems, up to 12 dB gain in the electrical signal-noise-ratio (SNR) is predicted with two direct-detection PIN photodetectors in strong atmospheric turbulence.

In optical receiver design, avalanche photodiodes (APDs) are widely used since they provide higher values of responsivity compared with PIN photodiodes. However, APDs also introduce additional randomness to the photodetection process. The characteristics of APD devices and the performance of APD-based receivers have been studied extensively [12–14]. Recently, the performance of PIN- and APD-based FSO receivers under the impact of different noise sources has been comprehensively studied in [15]. Additionally, the performance of APD-based FSO systems using pulse-position modulation (PPM) under the impact of turbulence was reported in [16]. Also, APD array receiver was proposed for optical communications using binary PPM and OOK modulations [17]. Additionally, analysis of the impact of the APD receiver on the performance of FSO systems using PPM with spatial

diversity have been reported by Cvijetic *et al.* [18, 19]. However, to our best knowledge, bit-error rate (BER) analysis of the FSO systems using BPSK-SIM and APD receiver has not been appeared in the literature.

In this paper, we therefore theoretically analyse the performance of APD-based BPSK-SIM/FSO systems over atmospheric turbulence channels taking into account APD shot noise, thermal noise and other system parameters. Log-normal and gamma–gamma distributions are used for modelling weak-to-moderate and moderate-to-strong atmospheric turbulence channels, respectively. The APD shot noise and thermal noise are modelled as additive white Gaussian noise. In addition, the channel capacity is derived considering various link conditions and system parameters. We comprehensively discuss the impact of transmitted power, turbulence strength, link span, bit rate, APD average gain and temperature on the system's BER and channel capacity. We found that, although the impact of turbulence is severe, a proper selection of APD average gain could significantly improve the system performance in both cases of turbulence channels.

The remainder of this paper is organised as follows. Section 2 describes the system model. BER and channel capacity analyses are presented in Sections 3 and 4, respectively. Section 5 presents the numerical analysis, and finally, Sections 6 concludes the paper.

2 System model

Fig. 1 shows the simple block diagram of the FSO system using BPSK-SIM and APD receiver. The information generated by a source is modulated onto a radio frequency (RF) subcarrier signal using BPSK scheme, in which binary 'one' and 'zero' are represented by two different phases 180° apart. The optical modulator modulates the intensity of light source, that is, a laser, by using the output signal of the BPSK modulator. The direction and the size of the laser beam are determined by the collimator or telescope in the transmitter. At the receiver, the incoming optical field is converted into an electrical signal by the direct-detection APD receiver. A standard RF coherent demodulator is employed to recover the source information.

2.1 Channel modelling

Denoting a, $P_0(t)$ and $X(t)$ as the channel attenuation, the transmitted signal intensity, the random process representing the signal scintillation caused by the atmospheric turbulence, the received optical intensity $P(t)$ can be expressed as

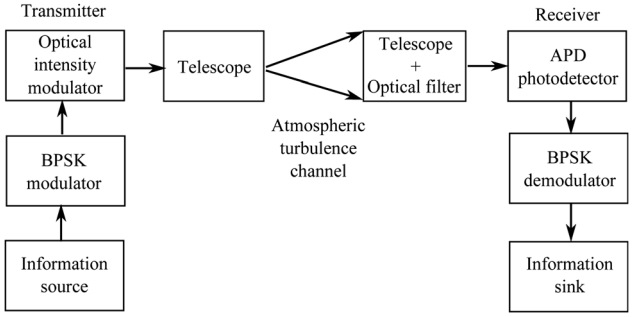

Fig. 1 *Block diagram of the FSO system using BPSK-SIM and APD receiver*

$$P(t) = aX(t)P_0(t) \tag{1}$$

The channel attenuation is caused by both molecular absorption and aerosol scattering suspended in the air. The total channel attenuation is given as [20]

$$a = \frac{A}{\pi(\phi L/2)^2}\exp(-\beta_\nu L) \tag{2}$$

where A, L, ϕ and β_ν are the area of the receiver's aperture, the link span, the angle of divergence in radian and the atmospheric extinction coefficient, respectively.

When the optical signal travels through the atmosphere free-space channel, it suffers from random intensity fluctuations, or scintillation effect, because of the atmospheric turbulence, even when propagation path is relatively short [21]. The scintillation effect is mainly caused by small-scale atmospheric temperature fluctuations that result in variations in the refractive index. The intensity fluctuations in the received signal consequently increase the BER, and thus degrade the system performance. When the turbulence is weak, it is generally accepted that the primary influence of turbulence $X(t)$ is a random process with log-normal distribution. Assuming that the average of the random process X is normalised to unity, its probability density function (pdf) is given by Majumdar [6]

$$f_X(x) = \frac{1}{\sqrt{2\pi}\sigma_s x}\exp\left[-\frac{\left(\ln x + \sigma_s^2/2\right)^2}{2\sigma_s^2}\right] \tag{3}$$

where σ_s^2 is the log intensity variance that depends on the channel's characteristics as given as [4, 6]

$$\sigma_s^2 = \exp\left[\frac{0.49\sigma_R^2}{\left(1+0.18d^2+0.56\sigma_R^{12/5}\right)^{7/6}} + \frac{0.51\sigma_R^2}{\left(1+0.9d^2+0.62d^2\sigma_R^{12/5}\right)^{5/6}}\right] - 1 \tag{4}$$

Here, $d = \sqrt{kD^2/4L}$, $k = 2\pi/\lambda$ is the optical wave number, L is the link span and D is the receiver's aperture diameter. The parameter σ_R^2 is the Rytov variance, and assuming plane wave propagation, it is given by

$$\sigma_R^2 = 1.23C_n^2k^{7/6}L^{11/6} \tag{5}$$

where C_n^2 is the altitude-dependent index of the refractive structure parameter determining the turbulence strength, Typically C_n^2 varies from 10^{-17} to 10^{-12} according to the strength of atmospheric turbulence [22].

In the strong turbulence regime, the log-normal distribution generates a significant difference with the experimental results [4]. The reason is that the log-normal pdf underestimates the behaviour of the tails as compared with experimental results. In this case, $X(t)$ can be modelled as a stationary random process with gamma–gamma distribution

doi: 10.1049/iet-com.2012.0600

and its pdf is given as [4, 6]

$$f_X(x) = \frac{2(\alpha\beta)^{(\alpha+\beta)/2}}{\Gamma(\alpha)\Gamma(\beta)} x^{(\alpha+\beta)/2-1} K_{\alpha-\beta}\left(2\sqrt{\alpha\beta x}\right) \quad (6)$$

where $\Gamma(.)$ is the gamma function, and $K_{\alpha-\beta}(.)$ is the modified Bessel function of the second kind and order $\alpha-\beta$. α and β are the pdf parameters describing the turbulence experienced by waves, and in the case of zero-inner scale they are given by [4]

$$\alpha = \left\{ \exp\left[\frac{0.49\sigma_R^2}{\left(1+1.11\sigma_R^{12/5}\right)^{7/6}} \right] - 1 \right\}^{-1}$$
$$\beta = \left\{ \exp\left[\frac{0.51\sigma_R^2}{\left(1+0.69\sigma_R^{12/5}\right)^{5/6}} \right] - 1 \right\}^{-1} \quad (7)$$

where the parameter σ_R^2 and d have been defined above. Fig. 2 shows pdfs for the gamma–gamma and log-normal cases with C_n^2 equal to 2×10^{-14} (moderate turbulence strength). It is important to note that the gamma–gamma model has a much higher density in both low and high amplitude regions, it therefore results in the better estimation of scintillation effect in the strong turbulence regime.

2.2 BPSK-SIM/FSO systems with APD photo-detector

In BPSK-SIM/FSO systems, the received optical power $P(t)$ can be written as

$$P(t) = aX(t)\frac{P_s}{2}\left[1 + m\cos\left(2\pi f_c t + a_i\pi\right)\right] \quad (8)$$

where P_s is the peak transmitted power of the laser beam in case of no turbulence, m is the modulation index, $a_i \in [0, 1]$ represents the ith binary data, and f_c is the subcarrier frequency. Assuming that the scintillation $X(t)$ varies slowly enough, the dc term $aX(t)P_s/2$ can be filtered out by a bandpass filter. The electrical signal at the output of the APD therefore can be written as

$$I(t) = m\Re\overline{g}\frac{P_s}{2}aX(t)\cos\left(2\pi f_c t + a_i\pi\right) + n(t) \quad (9)$$

where $\Re$ is the responsivity, $\overline{g}$ is the APD average gain and $n(t)$ is the receiver noise. For BPSK demodulation, the output signal $r(t)$ are demodulated by the reference signal $\cos(2\pi f_c t)$ as

$$r(t) = \overline{I(t)\cos\left(2\pi f_c t\right)}$$
$$= \begin{cases} \frac{1}{4}m\Re\overline{g}P_s aX(t) + \zeta(t) & \text{in the mark state} \\ -\frac{1}{4}m\Re\overline{g}P_s aX(t) + \zeta(t) & \text{in the space state} \end{cases} \quad (11)$$

where $\zeta(t)$ is the APD receiver noise caused by shot noise, thermal noise and dark current. Assume that the dark current is negligible, $\zeta(t)$ can be given by

$$\zeta(t) = i_{\text{Sh}}(t) + i_{\text{Th}}(t) \quad (12)$$

where $i_{\text{Sh}}(t)$ and $i_{\text{Th}}(t)$ is the shot noise and thermal noise, respectively. The thermal noise $i_{\text{Th}}(t)$ is a zero-mean stationary Gaussian random process with the variance given by Agrawal [23]

$$\sigma_{\text{Th}}^2 = \left(4k_{\text{B}}T/R_{\text{L}}\right)F_{\text{n}}\Delta f \quad (13)$$

where k_{B}, T, R_{L}, F_{n}, Δf denotes the Boltzmann constant, the receiver temperature in Kelvin degree, the APD's load resistance, the amplifier noise figure and the effective noise bandwidth, respectively. It is noted here that we use $\Delta f = R_{\text{b}}/2$, where R_{b} is the system bit rate.

As the scintillation causes the fluctuation in the received optical power, it also causes the uncertainty in the APD shot noise variance. As the matter of fact, the temporal correlation time of the atmospheric scintillation process is on the order of several milliseconds, which is much longer than a bit duration (less than a microsecond when the bit-rate of few ten Mb/s). We therefore can assume that the scintillation is constant over a short time period Δt; that is, $X(t)| = x$ for $t_0 \le t < t_0 + \Delta t$, where t_0 is a certain time. As a result, the instantaneous shot noise can be treated as a stationary Gaussian random process with the variance given by Agrawal [23]

$$\sigma_{\text{Sh}}^2 = 2q\overline{g}^2F_A\Re\left(\frac{m}{4}P_s ax\right)\Delta f \quad (14)$$

where q, F_A denote the electron charge and the excess noise factor, respectively. For a typical APD, F_A is given by $F_A = k_A\overline{g} + (1-k_A)(2-(1/\overline{g}))$, where k_A denotes the ionisation factor. Since shot noise and thermal noise are independent Gaussian random processes, the total variance of noise can be obtained simply by adding individual variances

$$\sigma_N^2 = \sigma_{\text{Sh}}^2 + \sigma_{\text{Th}}^2 \quad (15)$$

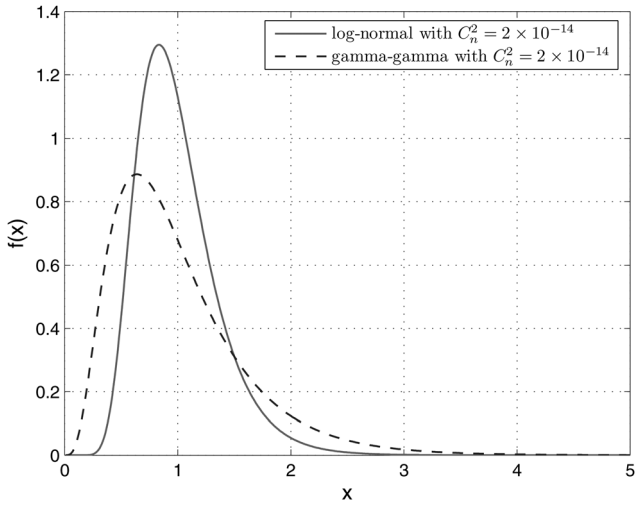

Fig. 2 *Log-normal and gamma–gamma pdfs*

3 BER analysis

In BPSK-SIM/FSO systems, the threshold level is fixed at the 'zero' mark thereby eliminating the need of an adaptive threshold as in OOK systems. For the equivalent transmitted data symbols, the BER is given by the probability of $r(t) < 0$ when a binary 'one' is sent. Therefore the following gives the unconditional BER

$$P_{\mathrm{e}} = \int_0^{\infty} P_{\mathrm{e}-i}(x) f_X(x)\,\mathrm{d}x \tag{16}$$

where $f_X(x)$ denotes the pdf of the random process caused by atmospheric turbulence, and $P_{\mathrm{e}-i}(x)$ denotes the instantaneous error probability that equals to the probability of $r(t) < 0$, in which we consider $r(t)$ in a Gaussian random process with instantaneous mean $(1/4)m\Re\bar{g}P_s ax$ and variance σ_N^2.

$$\begin{aligned} P_{\mathrm{e}-i}(x) &= \frac{1}{\sqrt{2\pi}\sigma_N}\int_{-\infty}^{0} \exp\left[-\frac{\left(r-(1/4)m\Re\bar{g}P_s ax\right)^2}{2\sigma_N^2}\right]\mathrm{d}r \\ &= Q\left(\frac{m\Re\bar{g}P_s a}{4\sigma_N}\,x\right) \end{aligned} \tag{17}$$

where from (13)–(15), the noise variance σ_N^2 is given by

$$\sigma_N^2 = 2q\bar{g}^2 F_A \Re\left(\frac{m}{4}P_s ax\right)\Delta f + \left(4k_B\frac{T}{R_L}\right)F_n\Delta f \tag{18}$$

and $Q(.)$ is the Gaussian Q-function with

$$Q(y) = \frac{1}{\sqrt{2\pi}}\int_y^{\infty}\exp\left(-\frac{t^2}{2}\right)\mathrm{d}t \tag{19}$$

3.1 Log-normal channel model

Substituting (17) and (3) into (16) we obtain the expression for the BER of the system

$$\begin{aligned} P_{\mathrm{e}} = &\int_0^{\infty} Q\left(\frac{m\Re\bar{g}P_s a}{4\sigma_N}\,x\right) \\ &\times\frac{1}{\sqrt{2\pi}\sigma_s x}\exp\left[-\frac{\left(\ln x+\sigma_s^2/2\right)^2}{2\sigma_s^2}\right]\mathrm{d}x \end{aligned} \tag{20}$$

Making the change of variable $y = \left(\ln x + \sigma_s^2/2\right)/\sqrt{2}\sigma_s$ we have

$$\begin{aligned} P_{\mathrm{e}} = &\frac{1}{\sqrt{\pi}}\int_{-\infty}^{\infty} Q\left[\frac{m\Re\bar{g}P_s a}{4\sigma_N}\exp\left(\sqrt{2}\sigma_s y-\sigma_s^2/2\right)\right] \\ &\times\exp\left(-y^2\right)\mathrm{d}y \end{aligned} \tag{21}$$

with

$$\begin{aligned} \sigma_N^2 = &2q\bar{g}^2F_A\Re\Delta f\frac{m}{4}P_s a\exp\left(\sqrt{2}\sigma_s y-\sigma_s^2/2\right) \\ &+\left(4k_B\frac{T}{R_L}\right)F_n\Delta f \end{aligned} \tag{22}$$

Using the approximation [24]

$$\int_{-\infty}^{\infty} g(y)\exp\left(-y^2\right)\mathrm{d}y \simeq \frac{1}{\sqrt{\pi}}\sum_{i=-N;i\neq 0}^{N} w_i g\left(y_i\right) \tag{23}$$

where w_i and y_i with $i = (-N, -N+1, ..., 1, 2, ..., N)$ are the weighting factors and the zeros of the Hermite polynomial, respectively, we can obtain a tractable expression of P_{e}, that is

$$P_{\mathrm{e}} \simeq \frac{1}{\sqrt{\pi}}\sum_{i=-N;i\neq 0}^{N} w_i Q\left[\frac{m\Re\bar{g}P_s a}{4\sigma_{N-i}}\exp\left(\sqrt{2}\sigma_s y_i-\sigma_s^2/2\right)\right] \tag{24}$$

with

$$\begin{aligned} \sigma_{N-i}^2 = &2q\bar{g}^2F_A\Re\Delta f\frac{m}{4}P_s a\exp\left(\sqrt{2}\sigma_s y_i-\sigma_s^2/2\right) \\ &+\left(4k_B\frac{T}{R_L}\right)F_n\Delta f \end{aligned} \tag{25}$$

3.2 Gamma–gamma channel model

For gamma–gamma channels the BER expression is given by

$$\begin{aligned} P_{\mathrm{e}} = &\int_0^{\infty} Q\left(\frac{m\Re\bar{g}P_s a}{4\sigma_N}\,x\right) \\ &\times\frac{2(\alpha\beta)^{(\alpha+\beta)/2}}{\Gamma(\alpha)\Gamma(\beta)}x^{(\alpha+\beta)/2-1}K_{\alpha-\beta}\left(2\sqrt{\alpha\beta x}\right)\mathrm{d}x \end{aligned} \tag{26}$$

where σ_N is given by (18). This BER can be evaluated numerically using Matlab's standard functions.

4 Channel capacity

Channel capacity (C_s) is the tightest upper bound on the amount of information that can be reliably transmitted over a communications channel. It can be derived as a function of the received optical signal, noise power, the modulation and the detection method. The channel capacity per symbol is defined as

$$C_s = \max I(U;V)\quad(\text{bit/symbol}) \tag{27}$$

where the maximisation is over all possible input probability distributions $\{P(u_i)\}$ on U, and $I(U, V)$ is the mutual information of the channel.

Assuming that the probabilities of receiving a binary 'one' or 'zero', when respectively a binary 'zero' or 'one' is sent, are equal; the channel can be regarded as a binary symmetric channel. The mutual information therefore can be given by

$$\begin{aligned} I(U;V) &= H(V) - H(V|U) \\ &= H(V) + P_{\mathrm{e}}\log_2 P_{\mathrm{e}} + \left(1-P_{\mathrm{e}}\right)\log_2\left(1-P_{\mathrm{e}}\right) \end{aligned} \tag{28}$$

where $H(.)$ is the entropy function and P_{e} is the BER of the system as defined in the previous section. As a result, the

doi: 10.1049/iet-com.2012.0600

channel capacity per symbol is given by

$$C_s = 1 + P_e \log_2 P_e + (1 - P_e)\log_2(1 - P_e) \quad (29)$$

5 Numerical analysis

In this section, using the previously derived formulations, we numerically analyse the BER of FSO systems employing BPSK-SIM and APD receiver over atmospheric turbulence channels. Unless otherwise noted, the system parameters and constants are listed in Table 1. For the receiver, we use typical parameters with $R_L = 1000\ \Omega$, $F_n = 2$, the responsivity $\Re = 1$ corresponding to an InGaAs APD receiver, and the optical wavelength of 1.55 μm [23]. The atmospheric extinction coefficient $\beta_v = 0.1$ dB/km, which is a typical value for clear air conditions [25], is selected. We also assume a typical value of the receiver's aperture diameter $D = 2$ cm [25]. Moreover, for the weak-to-moderate turbulence regime we use the log-normal, whereas the gamma–gamma model is used for the strong turbulence regime. The turbulence strengths $C_n^2 = 6 \times 10^{-15}$, $C_n^2 = 2 \times 10^{-14}$ and $C_n^2 = 5 \times 10^{-14}$ are selected for weak, moderate and strong turbulence channels, respectively.

A point of interest that naturally follows is the selection of APD average gain $\overline{g}$ that optimises the system performance. Figs. 3 and 4 show BER against the APD average gain for various levels of the turbulence strength C_n^2 and various values of the link span L, respectively. As expected, the performance can be optimised by an appropriate selection of APD average gain. Moreover, the optimal gain remains almost unchanged over the entire range of the turbulence strengths and the link spans. This optimal value is in the neighbourhood of 15. We observe clearly that the correct selection of APD gain plays a key role in receiver design.

In Fig. 5, we show BER as a function of APD average gain for various levels of the receiver noise temperature for a log-normal channel. We fix the peak transmitted power $P_s = 0$ dBm and the turbulence strength $C_n^2 = 2 \times 10^{-14}$. It is seen that the optimal gain varies significantly in accordance to the change of the noise temperature. In particular, when the noise temperature increases from 100 to 900 K, the optimal gain increases from $\overline{g} = 12$ to $\overline{g} = 23$. When the APD average gain exceeds 35, the thermal noise is dominated by APD shot noise. Since it is practically difficult to adaptively alter $\overline{g}$, when information about temperature is unknown or varies, the selection of higher $\overline{g}$ could guarantee more accurate estimation of the system's BER as the effect of thermal noise is negligible.

Table 1 System parameters and constants

Name	Symbol	Value
Boltzmann's constant	k_B	1.38×10^{-23} W/K/Hz
electron charge	q	1.6×10^{-19} C
modulation index	m	1
receiver noise temperature	T	300 K
APD load resistance	R_L	1000 Ω
amplifier noise figure	F_n	2
bit rate	R_b	2 Gb/s
ionisation factor	k_A	0.7 (InGaAs APD)
responsivity	$\Re$	1
receiver's aperture diameter	D	0.02 m
atmospheric extinction coefficient	β_v	0.1 dB/km
angle of divergence	ϕ	10^{-3} rad

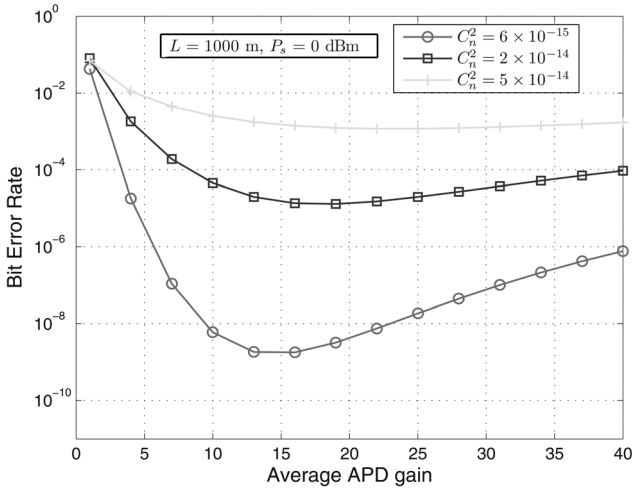

Fig. 3 *BER against APD average gain when $P_s = 0$ dBm, $L = 1000$ m, $T = 300$ K and $R_b = 2$ Gb/s for various levels of C_n^2*

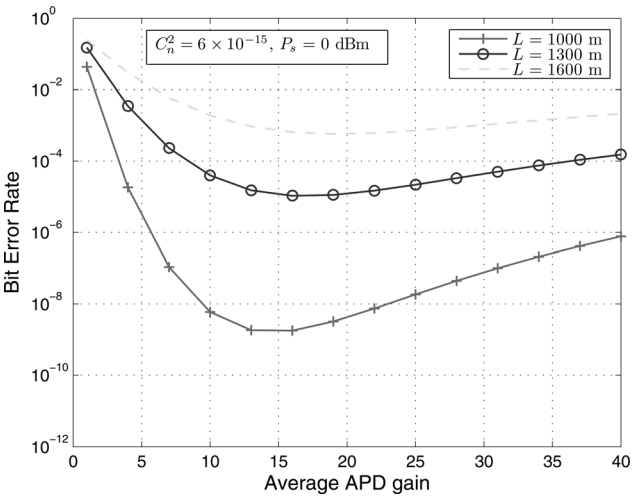

Fig. 4 *BER against APD average gain when $P_s = 0$ dBm, $C_n^2 = 6 \times 10^{-15}$, $T = 300$ K and $R_b = 2$ Gb/s for various levels of link span*

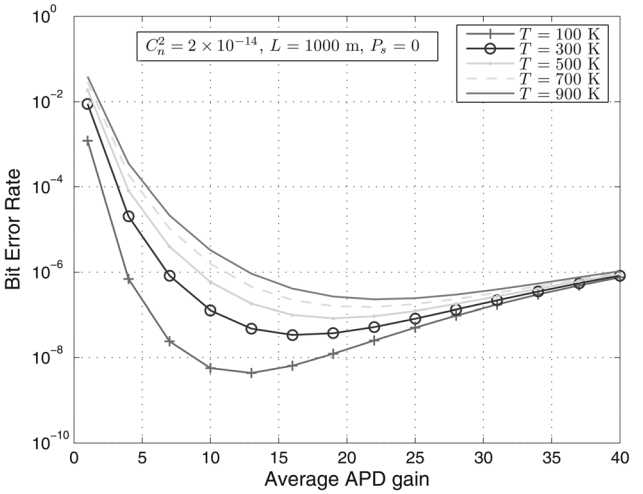

Fig. 5 *BER against APD average gain when $P_s = 0$ dBm, $L = 1000$ m, $C_n^2 = 2 \times 10^{-14}$ and $R_b = 2$ Gb/s for various levels of noise temperature*

In Fig. 6, the BER is presented as a function of the peak transmitted power for different levels of turbulence strength. As is evident, the increase in atmospheric turbulence results in an increase in the required power at the receiver to achieve the same performance. For instance, to achieve the performance of 10^{-8} in weak-to-moderate turbulence regime, the required peak transmitted power are –1 and 5 dBm for the turbulence strength value equal to 6×10^{-15} and 2×10^{-14}, respectively. In the strong turbulence regime, to achieve a reasonable performance, the required power increases dramatically, that is, peak transmitted power of 23 dBm is required at the BER = 10^{-8}.

Fig. 7 compares the performance of PIN- and APD-based FSO systems for different values of the link span in weak turbulence regime. Optical receivers that employ an APD can provide higher SNR because of the internal gain that increases the photocurrent by a multiplication factor $\overline{g}$ as shown in (9). Fig. 7 indicates that an APD-based system with optimal gain provides an approximate 10 dB improvement compared with a PIN-based one, highlighting the APD advantage. Furthermore, as is evident, system performance depends strongly on the link span L. More specifically, an increase in L by 500 m leads to an increase of the required power by approximately 4 dB to maintain the performance of 10^{-10}.

Fig. 8 shows the BER against turbulence strength for several values of bit rate for a weak turbulence channel. Note that the bandwidth Δf is treated as $\Delta f = R_b/2$, where R_b is the bit rate and the peak transmitted power is fixed to $P_s = -4$ dBm. This figure reveals that bit-rate adaptive systems could be introduced to de-emphasise the impact of turbulence. For example, when the turbulence strength increases from 4×10^{-15} to 1.3×10^{-14} the system should reduce the bit rate from 1 Gb/s to 200 Mb/s to maintain the BER of 10^{-9}.

Fig. 9 shows channel capacity versus peak transmitted power for $L = 1000$ m considering different levels of turbulence strength. It is intuitively clear that the higher turbulence strength leads to a reduction in the channel capacity. In the weak turbulence regime when $C_n^2 = 6 \times 10^{-15}$, the channel capacity can reach maximum value

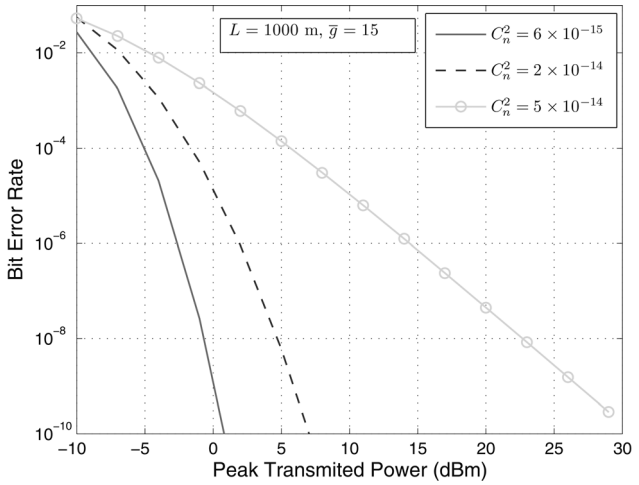

Fig. 6 *BER against peak transmitted power P_s (dBm) when $\overline{g} = 15$, $L = 1000$ m, $T = 300$ K and $R_b = 2$ Gb/s for various levels of turbulence strength C_n^2*

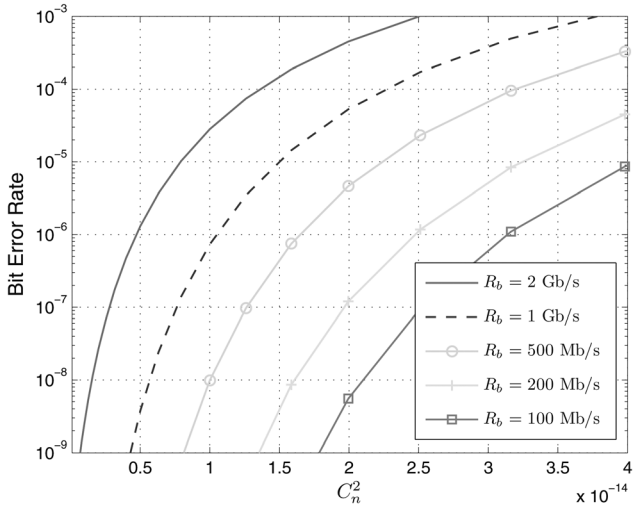

Fig. 8 *BER against turbulence strength for various levels of bit rate (log-normal channel)*

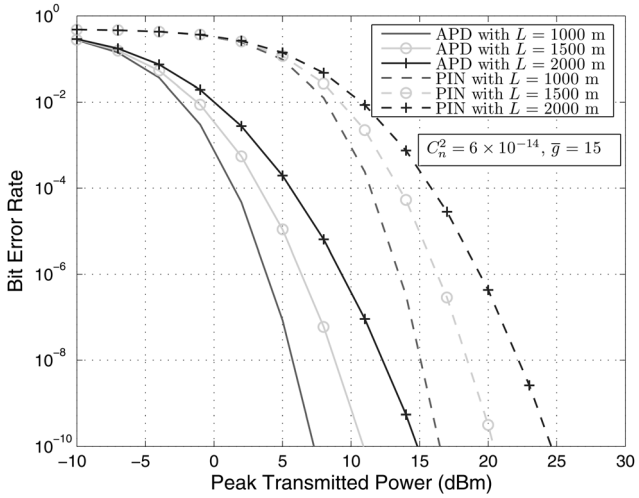

Fig. 7 *BER against peak transmitted power P_s (dBm) for APD receivers with $\overline{g} = 15$ and PIN receivers for various levels of link span*

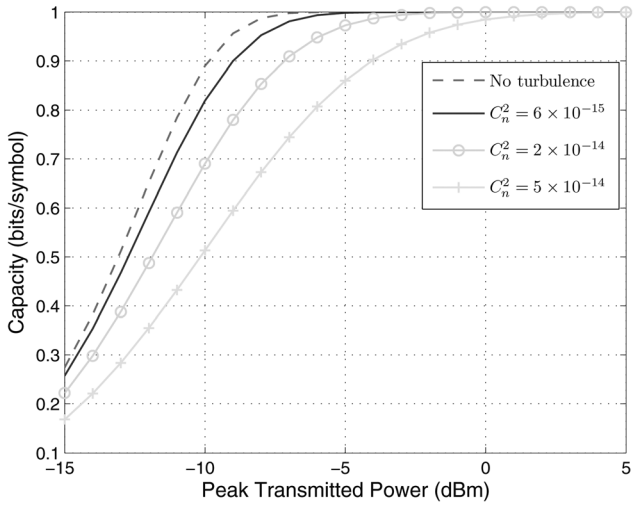

Fig. 9 *Channel capacity against peak transmitted power for various levels of turbulence strength*

doi: 10.1049/iet-com.2012.0600

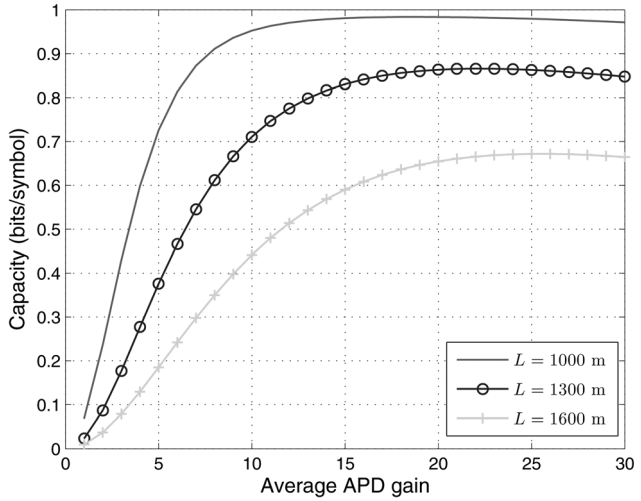

Fig. 10 *Channel capacity against APD average gain for different values of link span*

of 1 when $P_s \rightarrow -5$ dBm. In the strong turbulence regime, the capacity is about 0.88 when $P_s = -5$ dBm.

Finally, in Fig. 10 the channel capacity is presented as a function of the APD average gain for three different values of link span when $P_s = -7$ dBm, $T = 300$ K and $C_n^2 = 6 \times 10^{-15}$. We confirm again the significant effect of APD on the system performance. Furthermore, to achieve a reasonable capacity in a specific turbulence strength, the link span L should not be longer than a maximum value $L_{\max}$. For example, if we expect a capacity of 0.9 in this case, we should limit the link span to $L_{\max}$ of about 1300 m.

6 Conclusions

In this paper, using the log-normal and gamma–gamma distribution models to characterise the fluctuations of the optical signal, we have presented the performance analysis of FSO systems employing BPSK-SIM, when an APD receiver is used. The receiver noise, which comprises of APD shot noise and thermal noise, is modelled as additive white Gaussian noise. Both the system's BER and the channel capacity were theoretically derived taking into account various link conditions and receiver parameters. It was seen that the performance of such systems is severely affected by turbulence; however using APD receiver with optimal gain could significantly improve the system performance in both cases of turbulence channels. We also found that the optimal value of APD average gain remains the same for different levels of turbulence; nevertheless it varies significantly in accordance to the change of receiver noise temperature.

7 References

1 Ghassemlooy, Z., Popoola, W.O., Rajbhandari, S.: 'Optical wireless communications – system and channel modelling with Matlab' (CRC publisher, USA, 2012)

2 Nistazakis, H.E., Tsiftsis, T.A., Tombras, G.S.: 'Performance analysis of free-space optical communication systems over atmospheric turbulence channels', *IET Commun.*, 2009, **3**, pp. 1402–1409

3 Paraskevopoulos, A., Vucic, J., Voss, S.H., Swoboda, R., Langer, K.D.: 'Optical wireless communication systems in the Mb/s to Gb/s range, suitable for industrial applications', *IEEE/ASME Trans. Mech.*, 2010, **15**, (4), pp. 541–547

4 Al-Habash, M.A., Andrews, L.C., Phillips, R.L.: 'Mathematical model for the irradiance probability density function of a laser beam propagating through turbulent media', *Opt. Eng.*, 2001, **40**, (8), pp. 1554–1562

5 Bayaki, E., Schober, R., Mallik, R.K.: 'Performance analysis of MIMO free-space optical systems in gamma-gamma fading', *IEEE Trans. Commun.*, 2009, **57**, (11), pp. 3415–3424

6 Majumdar, A.K.: 'Free-space laser communication performance in the atmospheric channel', *J. Opt. Fiber Commun. Res.*, 2005, **2**, pp. 345–396

7 Popoola, W., Ghassemlooy, Z., Haas, H., Leitgeb, E., Ahmadi, V.: 'Error performance of terrestrial free space optical links with subcarrier time diversity', *IET Commun.*, 2012, **6**, p. 499

8 Shapiro, J.H., Harney, R.C.: 'Burst-mode atmospheric optical communication'. Proc. Nat. Telecommun. Conf. Record, New York, NY, USA, 1980, pp. 27.5.1–27.5.7

9 Huang, W., Takayanagi, J., Sakanaka, T., Nakagawa, M.: 'Atmospheric optical communication system using subcarrier PSK modulation', *IEEE Trans. Commun.*, 1993, **E76-B**, (9), pp. 1169–1177

10 Li, J., Liu, J.Q., Taylor, D.P.: 'Optical communication using subcarrier PSK intensity modulation through atmospheric turbulence channels', *IEEE Trans. Commun.*, 2007, **55**, (8), pp. 1598–1605

11 Popoola, W., Ghassemlooy, Z.: 'BPSK subcarrier intensity modulated free-space optical communications in atmospheric turbulence', *J. Lighwave Technol.*, 2009, **27**, (8), pp. 967–973

12 Conradi, J.: 'Distribution of gains in avalanche photodiodes – experimental results', *IEEE Trans. Electron. Devices*, 1972, **ED-6**, (6), pp. 713–718

13 Webb, D.: 'Properties of avalanche photodiodes', *RCA Rev.*, 1974, **35**, pp. 234–278

14 Sorensen, N., Gagliardi, R.: 'Performance of optical receivers with APD', *IEEE Trans. Commun.*, 1979, **COM-27**, (11), pp. 1315–1321

15 Xu, F., Khalighi, M., Bourenane, S.: 'Impact of different noise sources on the performance of PIN- and APD-based FSO receivers'. ConTEL 2011-11th Int. Conf. on Telecommun., Graz, Austria, June 2011, pp. 2110–2118

16 Kiasaleh, K.: 'Performance of APD-based, PPM free-space optical communication systems in atmospheric turbulence', *IEEE Trans. Commun.*, 2005, **53**, (9), pp. 1455–1461

17 Cole, M., Kiasaleh, K.: 'Receiver architectures for the detection of spatially correlated optical field using avalanche photodiode detector arrays', *Opt. Eng.*, 2008, **47**, (2), pp. 1–15

18 Cvijetic, N., Wilson, S.G., Brandt-Pearce, M.: 'Receiver optimization in turbulent free-space optical MIMO channels with APDs and Q-ary PPM', *IEEE Photonics Technol. Lett.*, 2007, **19**, (2), pp. 103–105

19 Cvijetic, N., Wilson, S.G., Brandt-Pearce, M.: 'Performance bounds for free-space optical MIMO systems with APD receivers in atmospheric turbulence', *IEEE J. Sel. Areas Commun.*, 2008, **26**, (3), pp. 3–12

20 Karp, S.: 'Optical channles: fibers, clouds, water and the atmosphere' (Plenum Press, 1988)

21 Zhu, X., Kahn, J.M.: 'Free-space optical communication through atmospheric turbulence channels', *IEEE Trans. Commun.*, 2002, **50**, (8), pp. 1293–1300

22 Goodman, J.W.: 'Statistical optics' (John Wiley, 1985)

23 Agrawal, G.P.: 'Fiber-optic communication systems' (John Wiley & Sons Inc., 2002, 3rd edn.)

24 Abramowitz, M., Stegun, I.A.: 'Handbook of mathematical functions, with formulas, graphs, and mathematical tables' (Dover, 1972, 9th edn.)

25 Ricklin, J.C., Hammel, S.M., Eaton, F.D., Lachinova, S.L.: 'Atmospheric channel effects on free-space laser communication', *J. Opt. Fiber Commun. Rep.*, 2006, **3**, pp. 111–158